Article

Discovery Medicine 2023; 35(178): 877–886
https://doi.org/10.24976/Discov.Med.202335178.83

Regulations of Exosomal-Transmitted *AFAP1-AS1* LncRNA on Ovarian Cancer Cell Migration and Invasion

Fuqun Zhou[1], Xiaohui Xu[1], Weidong Wei[2], Xiang Chen[1], Liying Sun[3,*]

[1]Deparment of Gynecology, Shaoxing Keqiao Maternal and Child Health Care Hospital, 312030 Shaoxing, Zhejiang, China
[2]Deparment of Gynecology, Shaoxing Maternal and Child Health Care Hospital, 312000 Shaoxing, Zhejiang, China
[3]Department of Pediatric Adolescent Gynecology, The Children's Hospital Zhejiang University School of Medicine, National Clinical Medical Research Center for Child Health and Disease, 310052 Hangzhou, Zhejiang, China
*Correspondence: sunliying6029@163.com (Liying Sun)
Published: 1 October 2023

Background: Adolescent ovarian cancer (OC) has high malignancy. Long non-coding RNAs (lncRNAs) have been implicated in the pathogenesis of various malignancies, but their role in adolescent OC remains poorly understood. This study aims to assess the modulatory role of Exosome-transmitted lncRNA Actin filament-associated protein 1 Antisense RNA 1 (*AFAP1-AS1*) on the activity of OC cells.

Methods: We recruited a cohort of 40 adolescent patients diagnosed with OC and a control group of 40 healthy individuals. Serum samples were collected from both groups prior surgical intervention. Exosomes from peripheral blood and ascites were collected via differential centrifugation. The expression levels of *AFAP1-AS1* in OC tissues and cell lines (IOSE-80, CAOV3, and SKOV3) were quantified using quantitative reverse-transcription polymerase chain reaction (qRT-PCR). The exosomal particle size and surface markers were characterized through nanoparticle tracking analysis and transmission electron microscopy. Furthermore, siRNA-mediated knockdown of *AFAP1-AS1* was performed in IOSE-80, CAOV3, and SKOV3 cell lines. Functional assays, including wound-healing experiments and Transwell migration assays, were conducted to evaluate cellular migration and metastasis.

Results: Our findings demonstrate that the expression of *AFAP1-AS1* is significantly upregulated in OC patients' serum exosomes and ascitic fluid, correlating with unfavorable pathological features such as advanced federation international of gynecology and obstetrics (FIGO) stage and larger tumor diameter. *In-vitro* experiments revealed that OC cell lines and primary human OC cells showed enhanced proliferation and metastasis when exposed to ascites-derived exosomes enriched in *AFAP1-AS1*. Importantly, we observed that *AFAP1-AS1* can be transmitted to neighboring cells via exosomal pathways. Additionally, exosomes isolated from ascites treated with siRNA targeting *AFAP1-AS1* can inhibit cellular migration and invasion.

Conclusions: Our data provide evidence for the oncogenic role of *AFAP1-AS1*, which is transmitted via exosomes. This finding has significant implications for understanding the molecular mechanisms of *AFAP1-AS1* in the pathogenesis of adolescent ovarian cancer.

Keywords: adolescent ovarian cancer; exosomes; lncRNA *AFAP1-AS1*; cell metastasis; cell migration; invasion

Introduction

Ovarian cancer (OC) is one of the common tumors of female reproductive organs [1,2]. The incidence of OC in children and adolescents, defined as females under 19 years old, is markedly lower compared to adults, constituting approximately 5%–10% of all cases [3]. Approximately 75%–90% of these cases in adolescents are benign, while the remaining 10%–25% are either malignant or borderline tumors [4–6]. Research indicates that despite its low incidence, the tumor's growth rate and malignancy are generally higher in adolescents than in adults. Notably, younger age is correlated with a higher proportion of malignant tumors [7]. The larger the tumor diameter, the greater the probability of malignancy [8].

Moreover, OC can also be associated with complications such as pedicle torsion, which can affect all age groups but is more frequent among restless children and adolescents. The incidence of pedicle torsion in this age group is around 4.9 per 100,000. Immediate surgical intervention is critical upon the diagnosis of torsion, or OC. However, if ovariectomy is performed at this time, it will affect their long-term life to a certain extent [9]. In recent years, immunotherapy has emerged as a promising treatment modality for various tumors [10]. Personalized immunotherapy strategies, tailored based on the tumor immune environment, are rapidly evolving, particularly those that involve delivering tumor-specific antigens or immunomodulators [11,12].

Exosome (Exo) are small extracellular vesicles (EVs) with a diameter ranging from 30 to 150 nm, generated via inward budding of the multivesicular body (MVB) within the endosomal pathway [13]. Originating from various cell types, exosomes can be released into various circulatory systems, such as the bloodstream, humoral system, and lymphatic system. They encapsulate a wide array of unique proteins, such as Tumor Susceptibility Gene 101 (TSG101) and the tetraspanin CD9, along with various nucleic acids like long non-coding RNAs (lncRNAs), microRNAs, mRNAs, and DNA [14,15]. Exosomes function as molecular couriers in intercellular communication, transmitting signaling molecules to other cells via receptor-ligand interactions or through membrane fusion [16]. Actin filament-associated protein 1 Antisense RNA 1 (*AFAP1-AS1*), a 6.8 kb lncRNA, is located on chromosome 4p16 1. However, its potential role as an exosome-carried molecule in the malignant transformation of adolescent OC remains underexplored. This study aims to investigate the regulatory effects of secreted *AFAP1-AS1* on adolescent OC cells' malignant phenotype and elucidate its mechanistic role in cellular migration and invasion.

Materials and Methods

Peripheral Blood Samples and Ascites Samples

A total of 40 adolescent OC patients who underwent surgery in Shaoxing Keqiao District Maternal and Child Health Hospital from June 2017 to September 2020 were enrolled for this study. None of the patients had received chemotherapy, immunotherapy, preoperative neoadjuvant radiotherapy, or other adjuvant therapies before surgery. Postoperative pathology analysis confirmed diagnosis of adolescent OC. As a control, 40 healthy subjects were also included in the study. From each participant, 2 to 3 mL of venous blood was collected. Informed consent was obtained from all subjects to collect and use ascites samples. This study was approved by the Ethics Committee of Ethics Committee of Keqiao District Maternal and Child Health Hospital (kqfby20200923), conducted in accordance with the official regulations for clinical research and the Declaration of Helsinki.

Extraction and Identification of Exosomes from Ascitic and Peripheral Blood Samples

The patient's blood samples were centrifuged at 1500 ×g for 15 min at 4 °C. The collected supernatant (2.5 mL serum) was centrifuged at 12,000 ×g for 30 min at 4 °C and then ultracentrifuged at 110,000 ×g for 2 h at 4 °C. The precipitate containing total exosomes was resuspended in 2.5 mL of phosphate-buffered saline (PBS), followed by ultracentrifugation at 110,000 ×g for 2 h at 4 °C. The precipitate was resuspended in 0.2 mL of PBS. After the collection of ascites specimens, the centrifugation procedure was the same as for peripheral blood specimens. Extracted exosomes were then validated using Western blot analysis with antibodies targeting exosomal markers CD63 (ab134045, Abcam, Cambridge, UK), CD9 (ab236630, Abcam, Cambridge, UK) and tumor susceptibility gene 101 protein (TSG101) (ab125011, Abcam, Cambridge, UK).

Isolation and Culturing of Human Primary OC Cells

OC tissues were washed 3 times in PBS containing 10% double antibodies for 5 minutes each. After removing impurities by rinsing the tissues in culture medium, they were fractionated into 0.5~1 mm^3 fragments and cultured in primary cell culture medium. The medium was replaced after 3 days during incubation at 37 °C in a 5% CO_2 atmosphere. Upon achieving a 80–90% cell density, cells were passaged using trypsin digestion until the fibroblasts were no longer observable to the naked eye and were able to continue passaging for stable growth. The resulting cell lines were authenticated using DNA-based methods and verified against the International Committee for Cell Line Accreditation (ICLAC) database for cross-contamination and misidentification.

Cell Culture

OC cells CAOV3 and SKOV3, and the human normal ovarian epithelial cell IOSE-80, were purchased from the Cell Bank of the Chinese Academy of Sciences. Cells were cultured under standard conditions: 5% CO_2, 37 °C, and 95% humidity. The culture medium used was Dulbecco's Modified Eagle Medium (DMEM)/F12 supplemented with 10% fetal bovine serum (FBS) (C0235, Invitrogen, Carlsbad, CA, USA). The genetic characteristics of all cell lines were identified using short tandem repeat (STR) analysis [17], all cells have been tested for mycoplasma without cell contamination.

Identification of Human Primary OC Cells by Immunofluorescence Assay

The primary OC cells were cultured to log phase and enzymatically digested using 0.4% membrane protease. The cells were then seeded in six-well plates at 10,000 cells per well and incubated overnight at 37 °C in a 5% CO_2 environment. The following day, cells were washed twice with phosphate-buffered saline (PBS) and fixed for 15 minutes using 2% paraformaldehyde. Cells were then blocked using 10% homologous secondary antibody serum for 30 minutes, followed by an overnight incubation at 4 °C with primary antibody. Post-incubation, cells were washed thrice with PBS for 3 minutes each and incubated for 1 hour with a secondary antibody. After adding 4'6-diamidino-2-phenylindole (DAPI) for 15 minutes and additional PBS washing, slides were prepared and observed under a fluorescence microscope (Olympus IX71, Shanghai Laishi Electronics, Shanghai, China).

Transmission Electron Microscopy

The exosome samples were prepared for transmission electron microscopy (TEM) using the negative staining

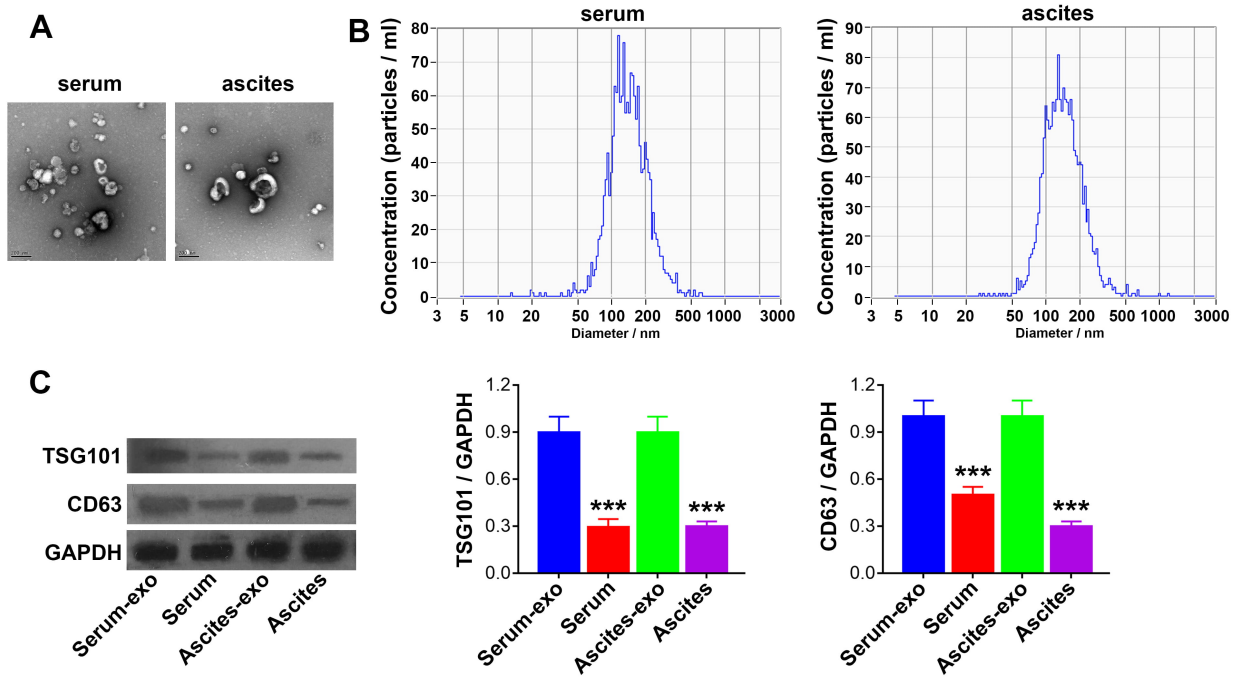

Fig. 1. Long non-coding RNA (lncRNA) Actin filament-associated protein 1 Antisense RNA 1 (*AFAP1-AS1*) level in exosomal specimens from patients with ovarian cancer (OC). (A,B) Transmission electron microscopy of the morphology of the patient's ascites, exosomes extracted from peripheral blood in a circular-like bilayer stereo membrane structure with nanoparticle tracking analysis of particle size ranging from 50–200 nm. Scale bar: 200 nm. (C) Western blot was performed to detect the expression of marker proteins in two cases of peripheral blood exosomes and two cases of exosomes extracted from ascites, and it was found that the Tumor Susceptibility Gene 101 (TSG101) and CD63 were positively expressed in the exosomes extracted from ascites. ***$p < 0.001$, compared with the serum-exosome (Exo) group/ascites-exo group. GAPDH, glyceraldehyde 3-phosphate dehydrogenase.

method, as previously described [18]. Briefly, 10 µL of exosome solution dissolved in PBS was added dropwise onto a 2 nm copper grid and air-dried at room temperature. Subsequently, 20 µL of 3% phosphotungstic acid was added for negative staining. Samples were observed and photographed using a MEGAVIEW G2 TEM system (HT7800, Thermo Fisher Scientific, Waltham, MA, USA).

Nanoparticle Tracking Analysis

Nanoparticle tracking analysis (NTA) was used to detect exosome particle size and concentration. The scattered light signals from exosomes were collected by microscopy, and the Brownian motion of exosomes was tracked and recorded to calculate the exosomes particle size and concentration. All samples were measured using NP100 membranes with 44.5 mm and 0.64 V parameters. The exosome solution was diluted 100 times and filtered through a 0.22 µm filter (033022, Nuowei Biology, Beijing, China), and the particle size distribution of exosomes was measured using the instrument.

RNA Extraction and qRT-PCR

RNA extraction and quantitative reverse-transcription polymerase chain reaction (qRT-PCR) detection of exosomal RNA were performed according to Trizol-LS instructions (10296028, Invitrogen, Carlsbad, CA, USA). A Thermo ultra-micro UV spectrophotometer was employed for concentration measurement. RNA samples were stored at –80 °C and reverse transcribed using the Prime Script™ one-step RT-PCR kit (RR064A, Takara, Shanghai, China). Reverse transcription reaction conditions: (i) 37 °C, 15 min; (ii) 85 °C, 5 s; (iii) 4 °C, continuous; the reaction solution obtained was diluted 10 times for subsequent experiments. qRT-PCR was performed on a Light Cycler 480 detection system (Verison 1.5, Roche, Basel, Switzerland), and the data obtained were analyzed by $2^{-\Delta\Delta CT}$, and each set of experiments was repeated three times. LncRNA *AFAP1-AS1* primer sequence: F:5′-AATGGTGGTAGGAGGGAGGA-3′; R:5′-CACACAGGGGAATGAAGAGG-3′.

Western Blot

Cells and exosomes were lysed using RIPA buffer (Bicinchoninic Acid Assay, BCA) containing a protease inhibitor Cocktail (Sigma, St. Louis, MO, USA). The lysates were incubated on ice for 30 minutes and centrifuged at 13,000 rpm for 10 minutes, and the supernatant was collected. Subsequently, a 10% sodium dodecyl sulfate-polyacrylamide gel electropheresis (SDS-PAGE) gel was prepared for electrophoresis to separate proteins. These proteins were then transferred onto polyvinylidene fluoride

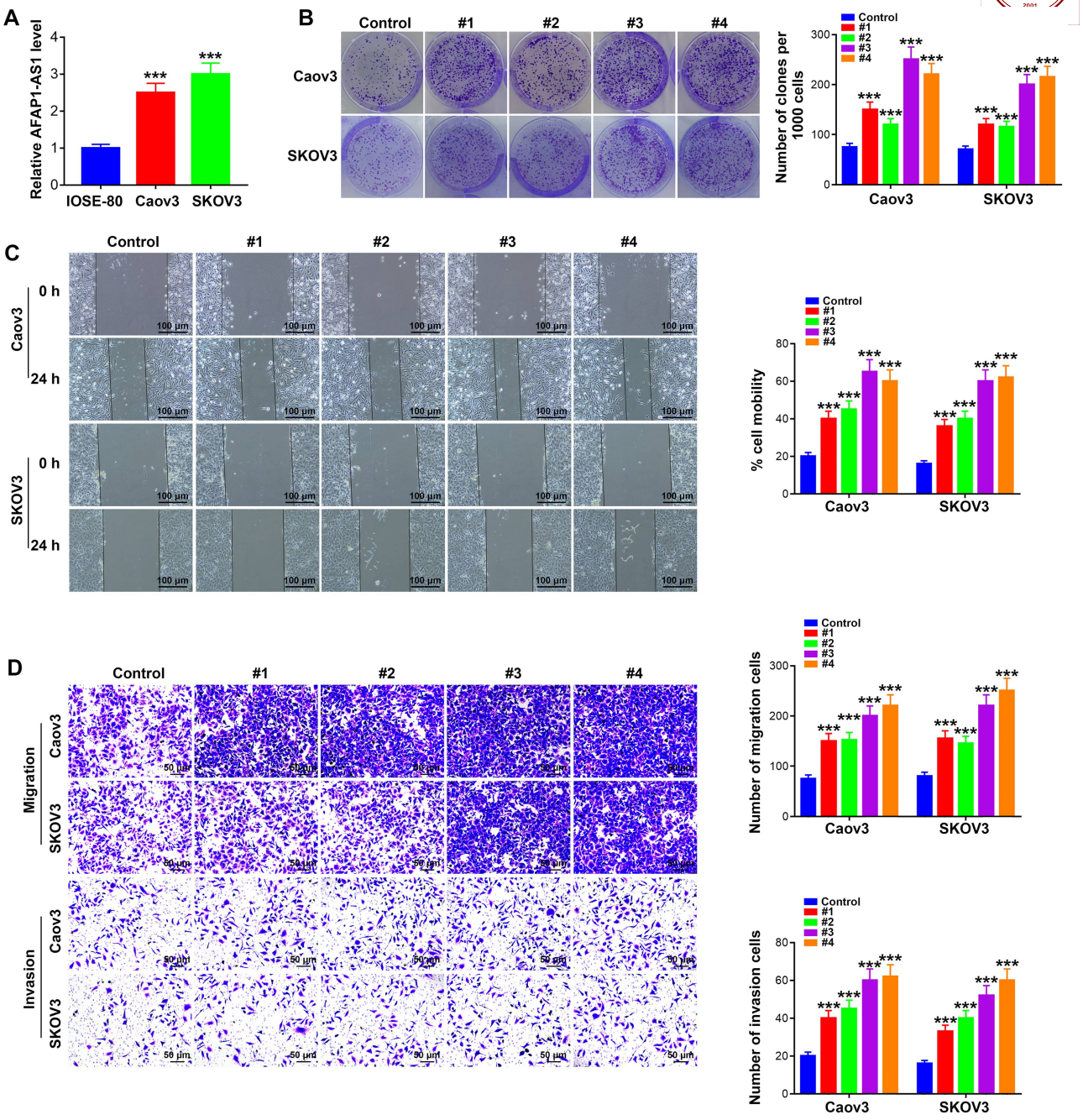

Fig. 2. Effects of ascites exosomes with different contents of lncRNA *AFAP1-AS1* on the phenotype of OC cells *in vitro*. Caov3 and SKOV3 cells were stimulated with ascites exosomes with different levels of lncRNA *AFAP1-AS1*, where labeled as low expression in #1 and #2 exosomes and high expression in #3 and #4 exosomes. (A) Detection of lncRNA *AFAP1-AS1* expression in the three cells with quantitative reverse-transcription polymerase chain reaction (qRT-PCR). (B) Results of colony formation after stimulation of Caov3 and SKOV3 cells by ascites exosomes. (C) Scratch assay to detect the migration ability and statistical histogram of cells after treatment of Caov3 and SKOV3 with ascites exosomes. The scale: 100 µM. (D) Transwell migration and invasion assay was applied to detect cells' migration and invasion ability after treatment of Caov3 and SKOV3 with ascites exosomes and statistical histograms. ***$p < 0.05$, compared with the Control (CON) group.

(PVDF) membranes. The membranes were blocked in 5% skimmed milk with Tris-buffered saline Tween-20 (TBST) and subjected to shaking for 1 h at room temperature. Primary antibodies for CD63 (ab134045, Abcam, Cambridge, UK), CD9 (ab236630, Abcam, Cambridge, UK), and TSG101 (ab125011, Abcam, Cambridge, UK) were added and incubated overnight at 4 °C. The next day, membranes were washed 3 times for 5 minutes each with TBST and then incubated with a horseradish peroxidase-labeled anti-rabbit secondary antibody (ab99757, 1:1000, Abcam, Cambridge, UK) for 1 h at room temperature. Finally, protein bands were visualized using an enhanced chemi-

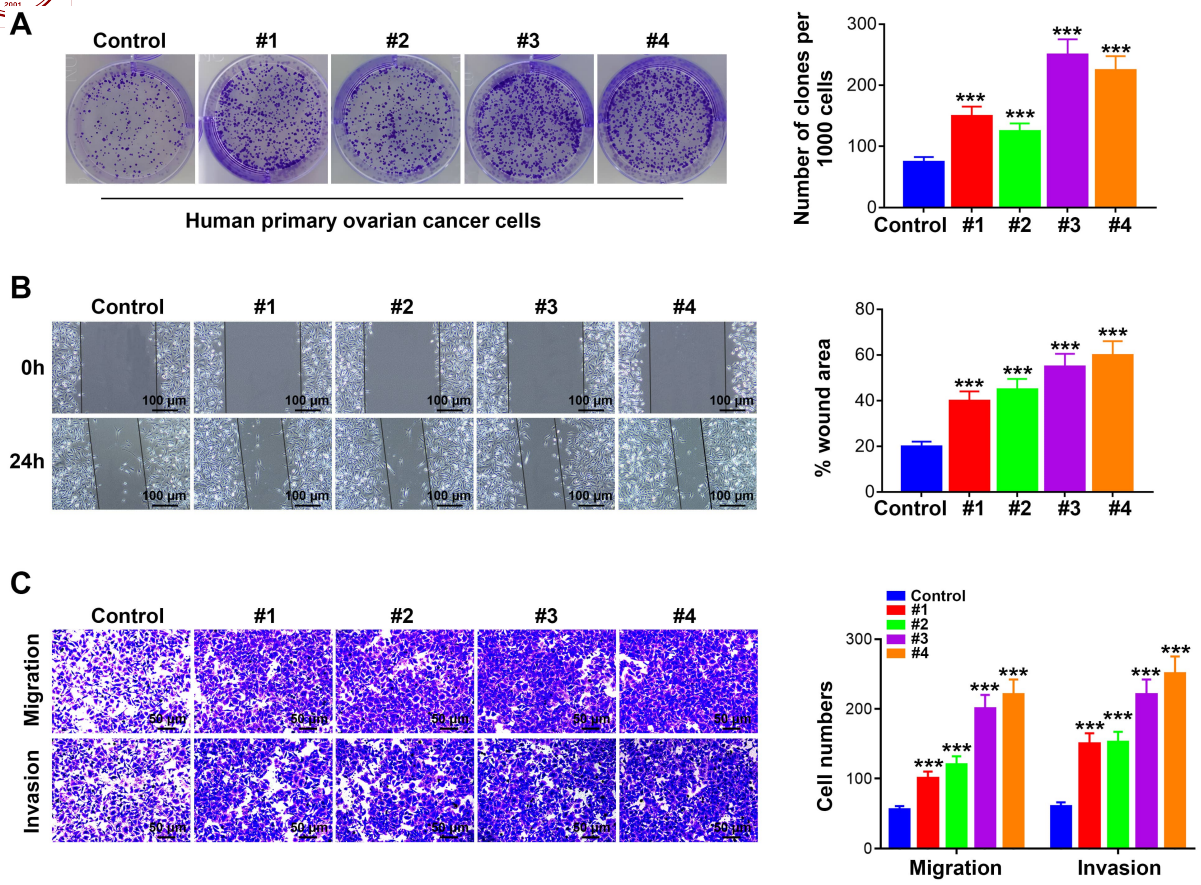

Fig. 3. Effects of ascites exosomes with different contents of *AFAP1-AS1* on the phenotype of primary OC cells. Stimulation of human primary OC cells by ascites exosomes with different levels of *AFAP1-AS1*. (A) Clonogenesis assay was applied to detect cell migration. (B,C) Scratch assay and Transwell migration assay were used to detect the migration of primary cancer cells. ***$p < 0.05$, compared with the CON group.

luminescence kit (Pierce, A38555, Thermo Fisher Scientific, MA, USA), and images were captured using Molecular Imager® ChemiDoc™ XRS+ with Image Lab™ software (V 6.0.1, Bio-Rad, Hercules, CA, USA). The ratio of the grayscale value of the target protein bands to that of glyceraldehyde 3-phosphate dehydrogenase (GAPDH) was calculated to determine the relative expression levels of the proteins.

PKH67 Staining

PKH67 (MINI67, Sigma-Aldrich, St. Louis, MO, USA) was used as a fluorescent dye for exosome staining. 100 μL of exosomes purified were mixed with PBS. Followed by addition to 1 mL of Diluent C (ICT6124, Saint Germain Biology, Shanghai, China) to prepare Diluent C-exosome suspension. 4 μL of PKH67 staining solution was added to 1 mL of Diluent C and mixed with the Diluent C-exosome suspension. The staining reaction was terminated by adding 2 mL of fetal bovine serum for 4 min at room temperature. Lastly, the exosomes were re-concentrated using a polyethylene glycol (PEG)-based method and resuspended in an appropriate volume of PBS.

Colony Formation Assay

OC cells treated with ascites exosomes were counted after trypsin digestion and seeded into six-well plates with 1000 cells per well. After 7–10 days of culturing, cells grew into individual colony visible to the naked eye. Cells were gently washed twice with PBS and fixed at room temperature for 20 min by adding 4% paraformaldehyde. Cells were washed twice with PBS and then stained with 0.1% crystal violet, left at room temperature for 30 min. After rinsing with tap water and air drying, the colony were photographed and analyzed. Experiment was performed in triplicate.

Cell Scratch Assay

Cancer cells were seeded in six-well plates and cultured so that they became covered by a single cell layer at near 100% density the next day. Cells were then washed twice with PBS to remove any non-adherent cells. A serum-free medium was added to inhibit cell proliferation, and scratches were made in the cell layer. Closure of these scratches was observed and photographed at 0 and 24 h. The area of cell closure was measured using Image-Pro Plus 6 software. The experiment was replicated three times for consistency.

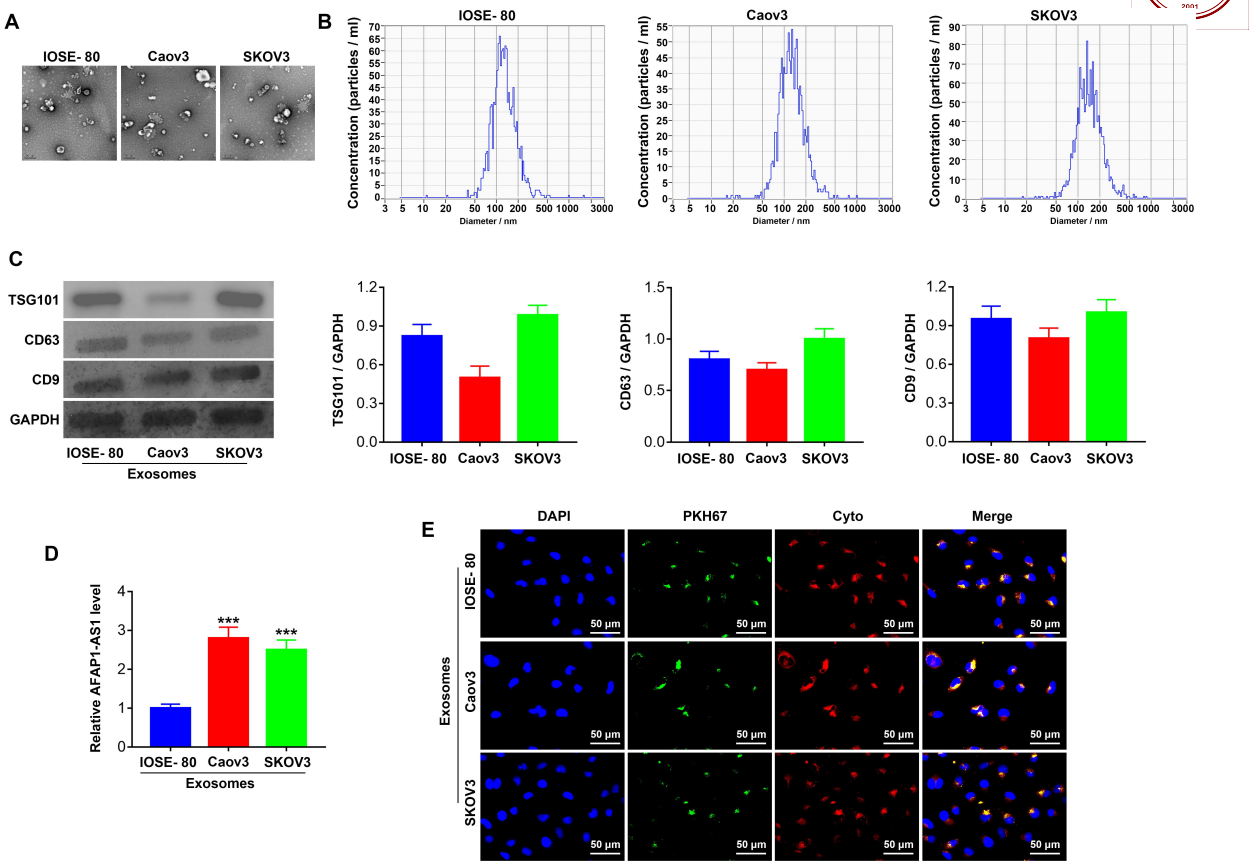

Fig. 4. ***AFAP1-AS1*** **transfer to recipient cells through exosomes.** (A) Transmission electron microscopy showed the images of exosomes secreted by IOSE-80, CAOV3, and SKOV3 cells, which showed a quasi-circular double-layer, three-dimensional membrane structure. Scale bar: 200 nm. (B) The diameter distribution of exosomes was tracked and analyzed by nanoparticles. (C) The expression of exosome marker proteins TSG101, CD63, and CD9 was detected by Western blot. (D) The expression difference of *AFAP1-AS1* in exosomes secreted by different cells was detected by qRT-PCR. (E) The uptake of exosomes by cells. Green represents PKH67 labeled exosomes, red represents cytoskeletal proteins, and blue represents 4'6-diamidino-2-phenylindole (DAPI) labeled nuclei. ***$p < 0.001$, compared with IOSE-80 group.

Transwell Assay

Cancer cells were digested with trypsin, counted, and resuspended in a serum-free DMEM/F12 medium. Two separate single-cell suspensions were prepared: one with 40,000 cells in 200 μL and another with 80,000 cells in 200 μL. These suspensions were placed in the upper chamber of a Transwell apparatus (8 mm diameter, Millipore) that was either uncoated or coated with Matrigel, for migration and invasion assays, respectively. The lower chamber was filled with a complete medium containing 10% fetal bovine serum. Following a 24 h incubation period, cells adhering to the upper surface of the Transwell membrane were carefully removed using a swab. Cells that had migrated to the lower chamber were fixed with formaldehyde, stained with 0.1% crystal violet, and observed under a microscope. Photographic documentation was performed, and cells in three randomly selected fields of view were counted. The average cell count from these fields was calculated. The experiment was repeated three times.

Statistical Analysis

All data were subjected to statistical analysis using SPSS 17.0 (IBM Corp., Chicago, IL, USA) and GraphPad Prism 5.0 software (GraphPad Software, Inc., San Diego, CA, USA). Numerical variables are presented as mean ± standard deviation. A *t*-test was performed to compare differences between two sets of data. For multiple comparisons, one-way analysis of variance (ANOVA) was utilized, and post-hoc tests were carried out when necessary. A *p*-value of less than 0.05 was considered statistically significant.

Results

AFAP1-AS1 Level in Exosomal Specimens from Patients with OC

To validate the efficiency of the ultracentrifugation method for exosome isolation, we employed transmission electron microscopy to characterize particle size and morphology. The method yielded a significant enrichment of

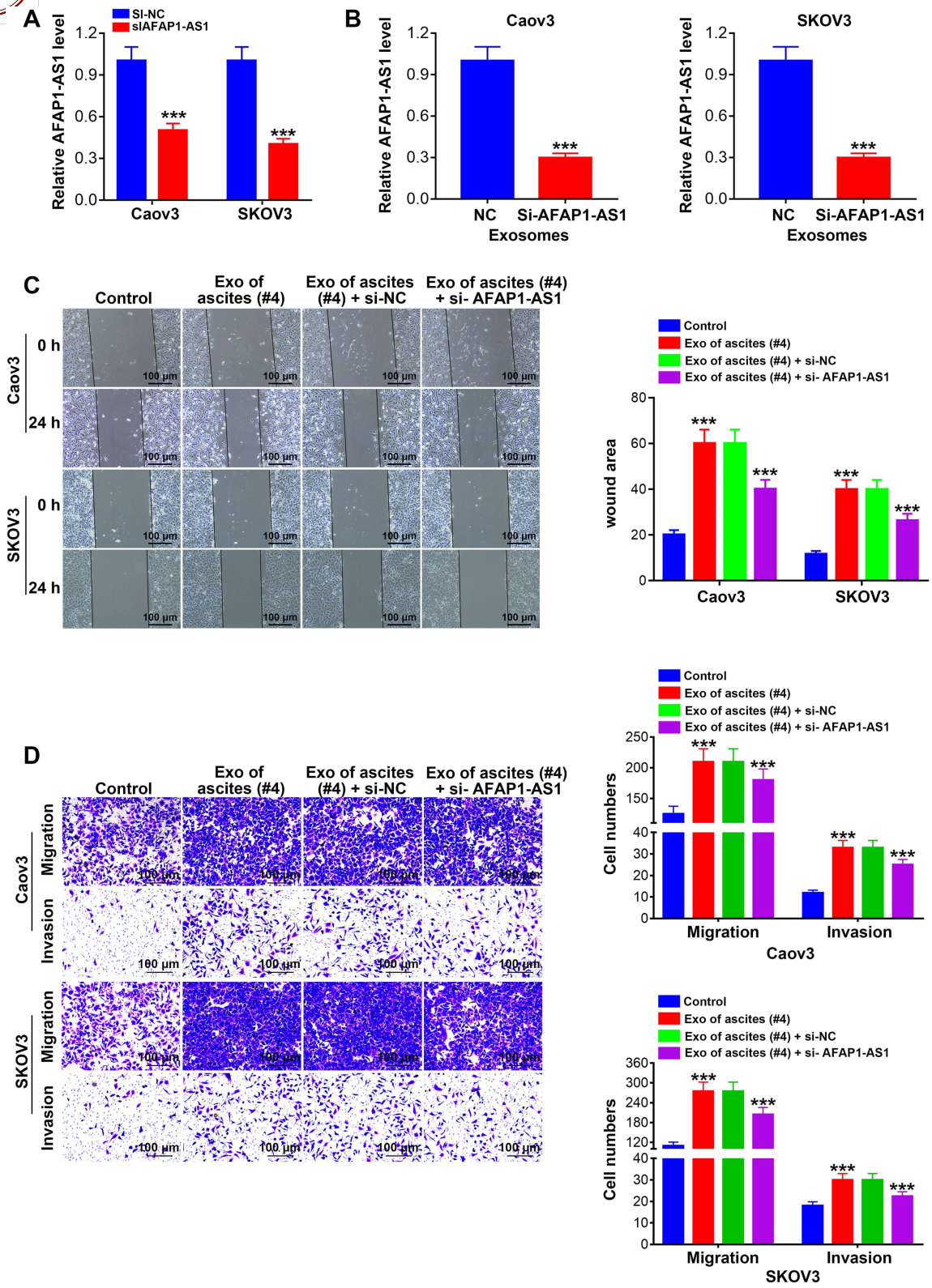

Fig. 5. Exosome-transmitted *AFAP1-AS1* promoted malignant phenotype in OC cells. (A) qRT-PCR was applied to detect the interference efficiency of si-RNA on *AFAP1-AS1* in Caov3 and SKOV3 cells. (B) qRT-PCR assay of *AFAP1-AS1* expression in exosomes secreted from si-*AFAP1-AS1* treated Caov3 and SKOV3 cells. Caov3 and SKOV3 cells were stimulated with higher *AFAP1-AS1* content of ascites exosomes (#4) and si-*AFAP1-AS1* or negative control (si-NC) and si-*AFAP1-AS1*-treated ascites-secreted exosomes. (C) Scratch assay was applied to detect the migration ability of Caov3 and SKOV3 cells. (D) Transwell assay for migration and invasion ability of Caov3 and SKOV3 cells. The scale: 100 μM. ***$p < 0.001$, compared with NC/CON group.

exosomes that exhibited a bilayer-like vesicular structure, suggesting high purity (Fig. 1A). Moreover, particle tracking analysis validated that the diameters of these exosomes ranged between 50–200 nm (Fig. 1B). We conducted Western blot analysis to validate the extracted exosomes further and successfully detected high levels of the exosomal markers TSG101 and CD63. Remarkably, these markers were significantly enriched in serum and ascitic fluid-derived exosomes compared to OC tissues (Fig. 1C), confirming the efficiency and quality of our exosome extraction method, including purity and high yield. Having established the robustness of our extraction method, we next delved into the functional implications of exosomal *AFAP1-AS1* in the context of ovarian cancer. An analysis of the correlation between exosomal *AFAP1-AS1* expression and the clinicopathological features of 40 OC patients revealed that high levels of serum and ascites *AFAP1-AS1* were associated with advanced federation international of gynecology and obstetrics (FIGO) stages and larger tumor sizes ($p < 0.05$, Tables 1,2). Hence, ascitic fluid exosomes were chosen for further experiments.

Table 1. Relationship between the expression of serum exosome *AFAP1-AS1* and clinicopathological features in patients with OC (n, %).

Features	n = 40	*AFAP1-AS1*		*p* value	χ^2
		High (%)	Low (%)		
Age (year)				0.429	0.625
≤12	8	3	5		
13∼19	32	17	15		
FIGO stage				0.001	11.033
I	12	2	10		
II	8	3	5		
III	10	7	3		
IV	10	8	2		
Tumor diameter				<0.001	12.907
<10	15	2	13		
≥10	25	18	7		

FIGO, federation international of gynecology and obstetrics.

Effects of Ascites Exosomes with Varying AFAP1-AS1 Levels on the Phenotype of OC Cells in Vitro

The clinicopathological significance of *AFAP1-AS1* observed in the previous section necessitated further scrutiny of its functional impact on ovarian cancer cells. Thus, we treated Caov3 and SKOV3 cell lines with ascites exosomes containing variable levels of *AFAP1-AS1*. These were labeled as low expression in #1 and #2 exosomes and high expression in #3 and #4 exosomes (Fig. 2A). Subsequent clonogenic assays pointed to increased cancer cellular activity with rising levels of *AFAP1-AS1* (Fig. 2A,B). Furthermore, cell scratch and Transwell assays revealed a commensurate increase in cell migration and metastasis, respectively (Fig. 2C,D). The level of *AFAP1-AS1* was generally consistent with the extent of the increase, suggesting in the metastasis of OC cells, that *AFAP1-AS1* may do a vital impact.

Table 2. Relationship between the expression of ascites exosome *AFAP1-AS1* and clinicopathological features in patients with OC (n, %).

Features	n = 40	*AFAP1-AS1*		*p* value	χ^2
		High (%)	Low (%)		
Age (year)				0.429	0.625
≤12	8	5	3		
13∼19	32	15	17		
FIGO stage				<0.001	14.700
I	12	3	9		
II	8	1	7		
III	10	8	2		
IV	10	8	2		
Tumor diameter				8.640	0.003
<10	15	3	12		
≥10	25	17	8		

Effects of Ascites Exosomes with Different AFAP1-AS1 Contents on the Phenotype of Primary OC Cells

Clonogenic survival assays were employed and revealed a consistent increase in the cellular activity of the primary OC cells in line with elevated levels of *AFAP1-AS1* (Fig. 3A). In addition, cell scratch and Transwell assays detected increased cell metastasis (Fig. 3B,C). These results agree with those observed in OC cell lines, thus reinforcing the notion that *AFAP1-AS1* might play a pivotal role in driving the aggressive behavior of OC cells at various disease stages.

AFAP1-AS1 could be Transferred to Recipient Cells through Exosomes

Cell-secreted exosomes can be released into the culture medium. To demonstrate whether *AFAP1-AS1* exerts biological effects by incorporating into exosomes, we collected IOSE-80, Caov3, and SKOV3 cell culture supernatants and extracted exosomes from culture supernatants using the PEG method and kit purification. To validate that the isolated vesicles were indeed exosomes, transmission electron microscopy was used to confirm their characteristic morphology (Fig. 4A,B). The expression of exosomal marker proteins TSG101, CD63 and CD9 was detected by Western blot and the exosomes were found to be positive (Fig. 4C). Subsequent analyses aimed to understand the exosomal *AFAP1-AS1* content in different cell lines. Interestingly, the Caov3 and SKOV3 cell lines secreted exosomes with substantially higher *AFAP1-AS1* content when compared to IOSE-80 cells (Fig. 4D). To detect whether the exosomes entered the cells, we used PKH67 staining to label the exosomes, DAPI to label the nucleus, and cytoskele-

tal staining. The exosomes secreted from IOSE-80, Caov3, and SKOV3 cells were co-cultured with IOSE-80 for 24 h, and the exosomes were seen to emit bright green fluorescence around the nucleus under fluorescence inverted microscopy (Fig. 4E), indicating that the exosomes could be taken up by the cells.

Exosome-Transmitted AFAP1-AS1 Promotes Malignant Phenotype in OC Cells

To precisely quantify the levels of *AFAP1-AS1* in OC cells, we utilized siRNA interference targeting this lncRNA. Caov3 and SKOV3 cells were transfected with either si-*AFAP1-AS1* or negative control (si-NC). The efficacy of the siRNA-mediated knockdown was subsequently assessed using qRT-PCR 24 hours post-transfection. The results indicated a marked reduction in the *AFAP1-AS1* expression levels in cells treated with si-*AFAP1-AS1* compared to the si-NC group (Fig. 5A). Exosomes were subsequently harvested from the culture supernatants of the si-NC and si-*AFAP1-AS1*-treated Caov3 and SKOV3 cells. qRT-PCR analysis revealed a significant decrease in the *AFAP1-AS1* content within the exosomes secreted by the si-*AFAP1-AS1*-transfected cells relative to the control group (Fig. 5B). The reduced *AFAP1-AS1* levels in exosomes made us question the downstream effects on cellular phenotype. Caov3 and SKOV3 cells were exposed to ascites-derived exosomes with varying *AFAP1-AS1* contents to address this. The experimental groups were designated as follows: Control (CON), Exo of ascites (#4), Exo of ascites (#4)+si-NC, and Exo of ascites (#4)+si-*AFAP1-AS1*. Using wound-healing assays, we found that cells treated with low *AFAP1-AS1*-containing exosomes exhibited reduced migration (Fig. 5C). Furthermore, Transwell assays corroborated these findings by demonstrating that diminished levels of exosomal *AFAP1-AS1* led to a significant inhibition of cellular invasion capabilities (Fig. 5D).

Discussion

The incidence of ovarian tumors among children and adolescents with gynecological diseases has gradually increased in recent years [19,20]. Exosomes released from tumor cells can transport oncogenes to paraneoplastic or less invasive cells and induce their tumorigenic and metastatic phenotypes, thus promoting cancer progression [21,22]. Long non-coding RNAs (lncRNAs) add another layer to this complex scenario. They modulate various biological processes, from chromatin remodeling to cell cycle regulation, either enhancing or inhibiting tumorigenesis, however, it remains unknown whether this lncRNA is delivered via exosomes in adolescent OC [23,24].

Our work extends this understanding by demonstrating that *AFAP1-AS1*, previously noted for its role in various malignancies, is transported via exosomes in adolescent OC. Several lncRNAs have been identified as pivotal in the metastasis and progression of different cancer types, such as LINC02273 in breast cancer and AOC4P in gastric cancer [25,26]. Similarly, our findings indicate an upregulation of *AFAP1-AS1* in juvenile OC tissues and cells, implicating this particular lncRNA in OC progression.

Continuing from the differential impact of *AFAP1-AS1* levels in exosomes on OC cell phenotype, we expand our discussion to other exosome-carried lncRNAs. For example, exosomal lncRNAs like UFC1 and RP11-838N2.4 in non-small cell lung cancer have been shown to regulate cellular multiplication and drug resistance [27,28]. Normal bladder epithelial cells release exosomes containing lncRNA phosphatase and tensin homolog pseudogene 1 (PTENP1). After lncRNA PTENP1 is transported to bladder cancer cells through exosomes, the occurrence of malignant phenotype is alleviated [29]. Our study found significantly elevated levels of *AFAP1-AS1* in ascites-derived exosomes and peripheral blood serum. Furthermore, these exosomes influenced the phenotype of primary OC cells and established OC cell lines, emphasizing the functional role of *AFAP1-AS1* in OC.

Given the phenotypic changes observed in OC cells upon *AFAP1-AS1* modulation, the diagnostic and therapeutic potentials of exosomal lncRNAs cannot be overlooked. Research into the mechanisms of exosomal lncRNAs has already shown promising avenues for clinical cancer treatment [30,31]. However, limitations persist. The precise molecular mechanisms through which *AFAP1-AS1* exerts its effects in OC remain an open question, as do *in vivo* verifications of its role in adolescent OC.

Conclusions

In conclusion, we observed a substantial increase in *AFAP1-AS1* levels in serum samples and OC cell lines. Moreover, our data demonstrate that this lncRNA can be shuttled between cells via exosomes, thereby influencing OC progression. Lower levels of exosomal *AFAP1-AS1* were found to inhibit OC cell migration and invasion. These findings underline the pivotal role of *AFAP1-AS1* in OC and suggest its potential as a diagnostic marker and therapeutic target in adolescent OC.

Availability of Data and Materials

The data used to support the findings of this study are available from the corresponding author upon request.

Author Contributions

FQZ contributed to the conception of the study manuscript preparation and have substantial contributions to the conception. XHX and XC contributed significantly to analysis and manuscript preparation. WDW performed the collection of laboratory data and the analysis. LYS performed the data analysis with constructive discussion. FQZ, WDW, XC and LYS revising it critically for important intellectual content. All authors have reviewed and ap-

proved the final manuscript. All authors have participated sufficiently in the work and agreed to be accountable for all aspects of the work.

Ethics Approval and Consent to Participate

This study was approved by the Ethics Committee of Ethics Committee of Keqiao District Maternal and Child Health Hospital (kqfby20200923), conducted in accordance with the official regulations for clinical research and the Declaration of Helsinki. Informed consent was obtained from all subjects to collect and use ascites samples.

Acknowledgment

Not applicable.

Funding

This research received no external funding.

Conflict of Interest

The authors declare no conflict of interest.

References

[1] Li RP, Li YW, Guo YZ. PD-1 and PD-L1 expression on the prognosis of ovarian cancer. Journal of Biological Regulators and Homeostatic Agents. 2019; 33: 1161–1166.

[2] Su JP, Liu HF, Zhang HL, He YJ, Nie Y. Effects of different degrees of depression on inflammatory response and immune function in patients with ovarian cancer. Journal of Biological Regulators and Homeostatic Agents. 2018; 32: 1225–1230.

[3] Lockley M, Stoneham SJ, Olson TA. Ovarian cancer in adolescents and young adults. Pediatric Blood & Cancer. 2019; 66: e27512.

[4] Blake EA, De Zoysa MY, Morocco EB, Kaiser SB, Kodama M, Grubbs BH, *et al*. Teenage pregnancy complicated by primary invasive ovarian cancer: association for oncologic outcome. Journal of Gynecologic Oncology. 2018; 29: e79.

[5] Wide A, Wettergren L, Ahlgren J, Smedby KE, Hellman K, Henriksson R, *et al*. Fertility-related information received by young women and men with cancer - a population-based survey. Acta Oncologica (Stockholm, Sweden). 2021; 60: 976–983.

[6] Stewart C, Ralyea C, Lockwood S. Ovarian Cancer: An Integrated Review. Seminars in Oncology Nursing. 2019; 35: 151–156.

[7] Kokoska ER, Keller MS, Weber TR. Acute ovarian torsion in children. American Journal of Surgery. 2000; 180: 462–465.

[8] Li GH, Yu JH, Yang B, Gong FC, Zhang KW. LncRNA LOXL1-AS1 inhibited cell proliferation, migration and invasion as well as induced apoptosis in breast cancer via regulating miR-143-3p. European Review for Medical and Pharmacological Sciences. 2019; 23: 10400–10409.

[9] Guthrie BD, Adler MD, Powell EC. Incidence and trends of pediatric ovarian torsion hospitalizations in the United States, 2000-2006. Pediatrics. 2010; 125: 532–538.

[10] Toribio-Vázquez C, Gómez Rivas J, Yebes A, Carrión DM, Quesada-Olarte J, Trelles CR, *et al*. Immunotherapy toxicity. Diagnosis and treatment. Archivos Espanoles De Urologia. 2020; 73: 906–917.

[11] Yang C, Xia BR, Zhang ZC, Zhang YJ, Lou G, Jin WL. Immunotherapy for Ovarian Cancer: Adjuvant, Combination, and Neoadjuvant. Frontiers in Immunology. 2020; 11: 577869.

[12] Barclay J, Creswell J, León J. Cancer immunotherapy and the PD-1/PD-L1 checkpoint pathway. Archivos Espanoles De Urologia. 2018; 71: 393–399.

[13] Maas SLN, Breakefield XO, Weaver AM. Extracellular Vesicles: Unique Intercellular Delivery Vehicles. Trends in Cell Biology. 2017; 27: 172–188.

[14] Diaz G, Bridges C, Lucas M, Cheng Y, Schorey JS, Dobos KM, *et al*. Protein Digestion, Ultrafiltration, and Size Exclusion Chromatography to Optimize the Isolation of Exosomes from Human Blood Plasma and Serum. Journal of Visualized Experiments: JoVE. 2018; 57467.

[15] Xu R, Rai A, Chen M, Suwakulsiri W, Greening DW, Simpson RJ. Extracellular vesicles in cancer - implications for future improvements in cancer care. Nature Reviews. Clinical Oncology. 2018; 15: 617–638.

[16] Wortzel I, Dror S, Kenific CM, Lyden D. Exosome-Mediated Metastasis: Communication from a Distance. Developmental Cell. 2019; 49: 347–360.

[17] McDermott AM, Baidouri H, Woodward AM, Kam WR, Liu Y, Chen X, *et al*. Short Tandem Repeat (STR) Profiles of Commonly Used Human Ocular Surface Cell Lines. Current Eye Research. 2018; 43: 1097–1101.

[18] Théry C, Amigorena S, Raposo G, Clayton A. Isolation and characterization of exosomes from cell culture supernatants and biological fluids. Current Protocols in Cell Biology. 2006; Chapter 3: Unit 3.22.

[19] Takayasu H, Masumoto K, Tanaka N, Aiyoshi T, Sasaki T, Ono K, *et al*. A clinical review of ovarian tumors in children and adolescents. Pediatric Surgery International. 2020; 36: 701–709.

[20] van Heerden J, Tjalma WA. The multidisciplinary approach to ovarian tumours in children and adolescents. European Journal of Obstetrics, Gynecology, and Reproductive Biology. 2019; 243: 103–110.

[21] Tai YL, Chen KC, Hsieh JT, Shen TL. Exosomes in cancer development and clinical applications. Cancer Science. 2018; 109: 2364–2374.

[22] Feng W, Dean DC, Hornicek FJ, Shi H, Duan Z. Exosomes promote pre-metastatic niche formation in ovarian cancer. Molecular Cancer. 2019; 18: 124.

[23] Qu CX, Shi XC, Bi H, Zhai LQ, Yang Q. LncRNA AOC4P affects biological behavior of gastric cancer cells through MAPK signaling pathway. European Review for Medical and Pharmacological Sciences. 2019; 23: 8852–8860.

[24] Abdi E, Latifi-Navid S, Latifi-Navid H, Safaralizadeh R. LncRNA polymorphisms and upper gastrointestinal cancer risk. Pathology, Research and Practice. 2021; 218: 153324.

[25] Xiu B, Chi Y, Liu L, Chi W, Zhang Q, Chen J, *et al*. LINC02273 drives breast cancer metastasis by epigenetically increasing AGR2 transcription. Molecular Cancer. 2019; 18: 187.

[26] Wang L, Cho KB, Li Y, Tao G, Xie Z, Guo B. Long Noncoding RNA (lncRNA)-Mediated Competing Endogenous RNA Networks Provide Novel Potential Biomarkers and Therapeutic Targets for Colorectal Cancer. International Journal of Molecular Sciences. 2019; 20: 5758.

[27] Zang X, Gu J, Zhang J, Shi H, Hou S, Xu X, *et al*. Exosome-transmitted lncRNA UFC1 promotes non-small-cell lung cancer progression by EZH2-mediated epigenetic silencing of PTEN expression. Cell Death & Disease. 2020; 11: 215.

[28] Li C, Ni YQ, Xu H, Xiang QY, Zhao Y, Zhan JK, *et al*. Roles and mechanisms of exosomal non-coding RNAs in human health and diseases. Signal Transduction and Targeted Therapy. 2021; 6: 383.

[29] Zheng R, Du M, Wang X, Xu W, Liang J, Wang W, *et al*. Exosome-transmitted long non-coding RNA PTENP1 suppresses bladder cancer progression. Molecular Cancer. 2018; 17: 143.

[30] Li Z, Meng X, Wu P, Zha C, Han B, Li L, *et al*. Glioblastoma Cell-Derived lncRNA-Containing Exosomes Induce Microglia to Produce Complement C5, Promoting Chemotherapy Resistance. Cancer Immunology Research. 2021; 9: 1383–1399.

[31] Sun Z, Yang S, Zhou Q, Wang G, Song J, Li Z, *et al*. Emerging role of exosome-derived long non-coding RNAs in tumor microenvironment. Molecular Cancer. 2018; 17: 82.